

## Thermodynamic Relations in Correlated Systems

Shinji Watanabe and Masatoshi Imada

Institute for Solid State Physics, University of Tokyo, 5-1-5, Kashiwanoha, Kashiwa, Chiba 277-8581

Several useful thermodynamic relations are derived from metal-insulator transitions, as generalizations of the Clausius-Clapeyron and Ehrenfest theorems. These relations hold in any spatial dimensions and at any temperatures. First, they relate several thermodynamic quantities to the slope of the metal-insulator phase boundary drawn in the plane of the chemical potential and the Coulomb interaction in the phase diagram of the Hubbard model. The relations impose constraints on the critical properties of the Mott transition. These thermodynamic relations are indeed confirmed to be satisfied in the cases of the one- and two-dimensional Hubbard models. One of these relations yields that at the continuous Mott transition with a diverging charge compressibility, the doublon susceptibility also diverges. The constraints on the shapes of the phase boundary containing a first-order metal-insulator transition at finite temperatures are clarified based on the thermodynamic relations. For example, the first-order phase boundary is parallel to the temperature axis asymptotically in the zero temperature limit. The applicability of the thermodynamic relations are not restricted only to the metal-insulator transition of the Hubbard model, but also hold in correlated systems with any types of phases in general. We demonstrate such examples in an extended Hubbard model with intersite Coulomb repulsion containing the charge order phase.

KEYWORDS: charge compressibility, doublon susceptibility, Mott transition, thermodynamic relation

## 1. Introduction

The interplay between the kinetic energy and the correlation effect for Fermion systems has been one of the most important subjects in the condensed matter physics. The interplay of quantum fluctuations and many-body effects can induce highly non-trivial phenomena. The metal-insulator transition driven by the electron correlation, which is called the Mott transition,<sup>1)</sup> offers such a prototype.<sup>2)</sup>

In the Mott transition, there are two control parameters: one is the chemical potential and the other is the bandwidth defined by the relative strength of the Coulomb interaction to the hopping integral. Controls by these two parameters are realized in a lot of examples in real materials as transition-metal compounds<sup>2)</sup> including cuprates which exhibits the high- $T_c$  superconductivity, organic materials<sup>3)</sup> and  $^3\text{He}$  systems.<sup>4)</sup>

Recently, critical exponents of the Mott transition through the bandwidth-control route in the phase diagram of temperature, pressure and magnetic field have been reported in  $(\text{V}_{1-x}\text{Cr}_x)_2\text{O}_3$ .<sup>5)</sup> The critical point was also identified in  $-(\text{ET})_2\text{CuN}(\text{CN})_2\text{Cl}$ .<sup>6)</sup> Although the measurements in  $(\text{V}_{1-x}\text{Cr}_x)_2\text{O}_3$  support the Ising universality<sup>5)</sup> predicted by G. Kotliar, et al.<sup>7(9)</sup> within the dynamical mean-field theory in the infinite spatial dimension,<sup>10)</sup> the measurements in  $-(\text{ET})_2\text{CuN}(\text{CN})_2\text{Cl}$  suggest a new aspect for the Mott transition.<sup>6)</sup> These circumstances indicate the importance of the theoretical study to clarify the basic properties of the Mott transition and the mutual relationship among the basic physical quantities near the Mott transition in finite spatial dimensions.

Theoretical studies of the Hubbard model by fully taking into account the spatial fluctuations in finite dimensions have been done by numerical calculations and an-

alytical methods. For the filling-control Mott transition, the continuous character with the diverging charge compressibility was clarified at zero temperature in the one-dimensional Hubbard model by the Bethe-Ansatz calculation<sup>11)</sup> and in the two-dimensional Hubbard model by the quantum Monte Carlo (QMC) calculations.<sup>12,13)</sup>

For the bandwidth-control Mott transition, the ground-state phase diagrams of the half-filled Hubbard models on the square lattice<sup>14)</sup> and the anisotropic triangular lattice<sup>15)</sup> have been determined by the path-integral renormalization group (PIRG) method.<sup>16,17)</sup> It has been suggested that the order of the Mott transitions changes from the first-order to continuous ones as the effect of magnetic frustration becomes large.

Recently, a new numerical algorithm, the grand-canonical path-integral renormalization group (GPIRG) method has been developed,<sup>18)</sup> which enables us to study the filling- and bandwidth-control Mott transitions in a unified framework. The GPIRG method has first made it possible to determine the ground-state phase diagram in the plane of the chemical potential and the Coulomb interaction of the square-lattice Hubbard model.<sup>18)</sup> It has been found that the V-shaped Mott insulator phase appears with the first-order bandwidth-control Mott transition at the corner of the V shape and the continuous filling-control Mott transition at the edges. The V-shaped structure has been shown to be consistent with the contrast found in the difference between the first-order bandwidth- and the continuous filling-control routes. This consistency is derived from the generalized Clausius-Clapeyron and Ehrenfest relations between the slope of the metal-insulator boundary and physical quantities.<sup>18)</sup>

In this paper, we further study the thermodynamic relations. We show that a couple of general relations

between physical quantities hold at each case of the first-order and continuous Mott transitions. These relations are again derived from the Clausius-Clapeyron and Ehrenfest relations and hold at any spatial dimensions and at any temperatures. We derive the thermodynamic relations between the charge compressibility and the doublon susceptibility for the continuous Mott transition, where the doublon susceptibility is shown to diverge when the charge compressibility diverges. The relations impose constraints on the shapes of phase diagrams.

The organization of this paper is as follows: In §2, the basic physical quantities for filling- and bandwidth-control routes are defined. The thermodynamic relations between the slope of the phase boundary and the physical quantities are derived for each case of the first-order and continuous Mott transitions. In §3, it is shown that they are actually satisfied in analytic forms obtained in the one- and two-dimensional Hubbard models. In §4, the thermodynamic relations are extended to finite temperatures. The constraints on the shapes of the phase diagram for the finite-temperature first-order transition are classified by using the thermodynamic relations. In §5, an application to other systems is demonstrated by taking an example of an extended Hubbard model with intersite Coulomb repulsion. We summarize the paper in §5.

## 2. Derivation of thermodynamic relations

### 2.1 Basic physical quantities for filling- and bandwidth-control routes

The Hubbard model which we consider is

$$H = \sum_{i,j} t_{ij} c_{i\uparrow}^\dagger c_{j\uparrow} + c_{i\downarrow}^\dagger c_{j\downarrow} - \mu \sum_i n_i + U \sum_i n_{i\uparrow} n_{i\downarrow}, \quad (1)$$

where  $c_i^\dagger$  ( $c_i$ ) is the annihilation (creation) operator on the  $i$ -th site with spin and  $n_i = c_{i\uparrow}^\dagger c_{i\uparrow}$  in the  $N$ -lattice system. Here,  $t_{ij}$  is the transfer integral and in this paper, the nearest-neighbor transfer is taken as the energy unit. In eq. (1)  $\mu$  is the chemical potential and  $U$  is the Coulomb interaction.

The electron filling  $n$  and the double occupancy  $D$  are defined by the first derivative of the Hamiltonian as

$$n = \frac{1}{N} \frac{\partial \langle H \rangle}{\partial \mu} = \frac{1}{N} \sum_{i=1}^N \langle n_i \rangle; \quad (2)$$

$$D = \frac{1}{N} \frac{\partial \langle H \rangle}{\partial U} = \frac{1}{N} \sum_{i=1}^N \langle n_{i\uparrow} n_{i\downarrow} \rangle = \frac{1}{N} \sum_{i=1}^N \langle n_{i\uparrow} \rangle \langle n_{i\downarrow} \rangle; \quad (3)$$

where  $\langle \dots \rangle$  represents the ground-state expectation value or the thermal average at finite temperature.

The charge compressibility  $\kappa_c$  and the doublon susceptibility  $\chi_D$  are defined, respectively, by the second

derivative of the Hamiltonian as

$$\kappa_c = \frac{1}{N} \frac{\partial^2 \langle H \rangle}{\partial \mu^2} = \frac{\partial n}{\partial \mu}; \quad (4)$$

$$\chi_D = \frac{1}{N} \frac{\partial^2 \langle H \rangle}{\partial U^2} = \frac{\partial D}{\partial U}; \quad (5)$$

### 2.2 The case where the phase boundary $U(\mu)$ has finite slope $U = U(\mu)$

#### 2.2.1 First-order-transition case

Although the following derivation of eq. (8) has been given in ref.<sup>18)</sup> we show here it for the self-contained description. Let us consider the ground state, although the results described below hold at finite temperatures, as will be mentioned in §4. The ground-state energy is expanded by  $\mu$  and  $U$ :

$$E(\mu, U) = E_I(\mu, U) + \frac{\partial E_I}{\partial U} U + \frac{\partial E_I}{\partial \mu} \mu + O(\mu^2, U^2); \quad (6)$$

In the  $-U$  phase diagram, along the metal-insulator-transition boundary, the energies of the metal and insulator phases should be the same because of the coexistence:

$$E_I(\mu, U) = E_M(\mu, U) \\ = E_I(\mu, U) + \frac{\partial E_I}{\partial U} U + \frac{\partial E_I}{\partial \mu} \mu = E_M(\mu, U) + \frac{\partial E_M}{\partial U} U + \frac{\partial E_M}{\partial \mu} \mu \\ = 0; \quad (7)$$

where subscripts  $I(M)$  represent that the expectation value is taken in the insulating (metallic) ground state. If the first-order metal-insulator transition occurs, the slope of the transition line in the  $-U$  phase diagram is determined by the ratio of the jump of filling and double occupancy. Namely, from eq. (6) and eq. (7) the following equation is derived:

$$\frac{U}{D_I} = \frac{n_I - n_M}{D_M - D_I}; \quad (8)$$

#### 2.2.2 Continuous-transition case

Let us consider the phase diagram in the  $-U$  plane in the ground state,  $T = 0$ . If the continuous metal-insulator transition occurs and the slope of the transition line is finite in the  $-U$  plane, the double occupancy is expanded by  $\mu$  and  $U$ , as follows:

$$D(\mu, U) = D_I(\mu, U) + \frac{\partial D_I}{\partial U} U + \frac{\partial D_I}{\partial \mu} \mu + O(\mu^2, U^2); \quad (9)$$

Along the metal-insulator-transition boundary, the double occupancies at the metallic and insulating phases have the same value at  $(\mu, U)$  and  $(\mu + \delta\mu, U + \delta U)$ :

$$D_M(\mu, U) = D_I(\mu, U) \\ = D_M(\mu, U) + \frac{\partial D_M}{\partial U} U + \frac{\partial D_M}{\partial \mu} \mu = D_I(\mu, U) + \frac{\partial D_I}{\partial U} U + \frac{\partial D_I}{\partial \mu} \mu; \quad (10)$$

where the subscripts  $M(I)$  represent that the average  $\langle \dots \rangle$  in eq. (3) is calculated in the metallic (insulating)

state. By substituting eq. (9) to eq. (10), the slope of the metal-insulator-transition boundary is expressed as

$$\begin{aligned} \frac{U}{\partial n} &= \frac{\frac{\partial D}{\partial U} U_M}{\frac{\partial D}{\partial U} U_I}; \\ &= \frac{\frac{\partial D}{\partial U} U_M}{\frac{\partial D}{\partial U} U_I}; \end{aligned} \quad (11)$$

where  $(\partial D / \partial U)_I = 0$  and eq. (5) are used.

On the other hand, we can derive another expression of  $U =$  starting from the expansion of  $\ln g(\mu)$ . In the parallel discussion as above, the slope of the metal-insulator transition boundary is derived as

$$\frac{U}{\partial n} = \frac{c}{\frac{\partial n}{\partial U}}; \quad (12)$$

If  $(\partial n / \partial U)_U$  and  $(\partial D / \partial U)$  are continuous at  $(\mu; U)$ , the following relation holds:

$$\begin{aligned} \frac{\partial n}{\partial U} &= \frac{1}{N} \frac{\partial}{\partial U} \left( \frac{\partial H}{\partial \mu} \right)_U \\ &= \frac{1}{N} \frac{\partial}{\partial U} \left( \frac{\partial H}{\partial \mu} \right)_U = \frac{\partial D}{\partial U}. \end{aligned} \quad (13)$$

We then obtain

$$\frac{\partial n}{\partial U}^2 = \frac{\partial D}{\partial U}^2 = c \left( \frac{\partial D}{\partial U} \right)^2; \quad (14)$$

By applying this equation to the thermodynamic relations of eq. (11) and eq. (12), the following Theorem 1 is derived: When the metal-insulator transition is a continuous one with a finite and nonzero slope in the  $\mu$ - $U$  phase diagram, the divergence of the charge compressibility occurs simultaneously with the divergence of the doublon compressibility. If the slope of the phase boundary is zero,  $U = 0$ ,  $c \neq 1$ ,  $\partial D / \partial U \neq 1$  still holds, whereas the converse is not necessarily true.

It should be noted that Theorem 1 derived above holds irrespective of the spatial dimensionality. The conditions in which Theorem 1 holds are as follows: First, there exists a finite length of the continuous metal-insulator-transition boundary  $U(\mu)$  in the  $\mu$ - $U$  plane, where  $U(\mu) =$  exists. Second, the slope of the metal-insulator boundary is finite, i.e.,  $\partial U / \partial \mu < 1$ . If the metal-insulator transition takes place as the continuous one with the  $U$ -shaped structure as shown in Fig. 1 (a), the thermodynamic relation holds at any point of the transition line.

### 2.3 The case where the slope $\partial U / \partial \mu$ is not well defined

When the Mott-insulator phase has the V-shaped structure in the  $\mu$ - $U$  phase diagram as shown in Fig. 1 (b), the above discussion is not applied at the corner of the V-shaped boundary, which is the bandwidth-control Mott-transition point, since  $U =$  is not well defined at the point. The V-shaped Mott-insulator phase in the  $\mu$ - $U$  plane seems to appear actually in the Hubbard model on the square lattice for  $t^0/t = 0.2$  with  $t$  and  $t^0$  being the nearest- and next-nearest-neighbor transfers.<sup>18)</sup> In

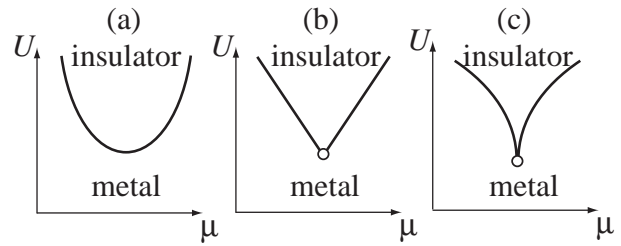


Fig. 1. Classification of the shapes of the phase diagrams in the plane of the chemical potential and the Coulomb interaction  $U$ : (a) U shape, (b) V shape, and (c) shape. The solid lines represent the continuous metal-insulator transition. In (b) and (c), the open circle located at the corner indicates the bandwidth-control Mott transition point to which the thermodynamic relation cannot be applied (see text).

this case, the first-order bandwidth-control Mott transition at the corner is compatible with the continuous filling-control Mott transition at the edges. This offers an example that the corner of the V shape can have the different character of the transition from the edges.

In the one-dimensional Hubbard model without the next-nearest-neighbor hopping, the metal-insulator phase boundary has a shape of  $\exp(-2t/U)$  for the small- $U=t$  regime.<sup>19)</sup> In the Hubbard model on the square lattice without the next-nearest-neighbor hopping, the metal-insulator phase boundary is expected to have a shape of  $\exp(-2t/U)$  for the small- $U=t$  regime.<sup>20)</sup> Both systems with the perfect nesting have the essential-singular form of the phase boundary, which is classified into the  $\mu$ -shaped case as shown in Fig. 1 (c). This is categorized to the same class as the V-shaped case. Namely, the thermodynamic relation can be applied except for the corner of the  $\mu$ -shaped boundary.

### 3. Analytic form of doublon susceptibility

In this section, we derive some useful analytic forms of  $\partial n / \partial U$ ,  $\partial D / \partial U$  and  $\partial D / \partial \mu$  near the continuous Mott transition, starting from the analytic forms of  $c$  realized in the one- and two-dimensional Hubbard models, and examine the thermodynamic relations, eqs. (11), (12) and (13) derived in §2. In this section, we approach the transition point from the metallic side.

#### 3.1 Derivation in one- and two-dimensional Hubbard models

Let us consider the vicinity of the metal-insulator transition in the metallic side of the  $\mu$ - $U$  phase diagram. In the one-dimensional Hubbard model without next-nearest-neighbor hopping,<sup>11)</sup> and in the two-dimensional Hubbard models with<sup>13,18)</sup> and without<sup>12)</sup> the next-nearest-neighbor hoppings, the filling dependence of the chemical potential is proposed to be scaled as

$$= c \frac{1}{2}^2; \quad (15)$$

with  $1/n$  and a constant  $c$ . In the one-dimensional system, eq. (15) was derived by the Bethe-Ansatz analysis<sup>11)</sup> and in the two-dimensional system, eq. (15) was identified by the QMC calculations.<sup>12,13)</sup> Note that here

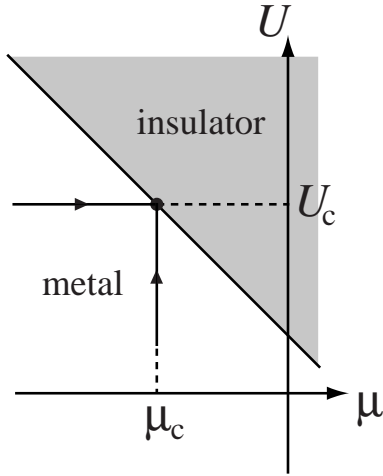


Fig. 2. Two ways of approaching the metal-insulator transition point denoted by the black circle at  $(\mu_c; U_c)$  in the  $U$ - $\mu$  plane: One is  $U \rightarrow U_c$  at  $\mu = \mu_c$  and the other is  $\mu \rightarrow \mu_c$  at  $U = U_c$ . These are the routes from the metallic side. The shaded area is the insulating phase and the solid line is the phase boundary.

we follow the notation of the chemical potential in refs.<sup>12,13</sup> to facilitate the comparison. From eq. (15), the doping rate is expressed by the chemical potential as

$$p = \frac{1}{2} \left( \frac{\mu}{\mu_c} \right)^2; \quad (16)$$

We need to consider the electron doping separately when the next-nearest neighbor hopping becomes nonzero causing the electron-hole asymmetry. Here, we consider the hole-doped case, although the following discussion can easily be extended to the electron-doped case. Then, the filling dependence of the charge compressibility is given by

$$\kappa = \frac{1}{1-n} = -; \quad (17)$$

By substituting eq. (16) to eq. (17), the chemical-potential dependence of the charge compressibility is given by

$$\kappa = \frac{r}{2} \left( \frac{\mu}{\mu_c} \right)^{1-2}; \quad (18)$$

To facilitate the discussion below, the most divergent terms of  $\partial D / \partial \mu$ ,  $\partial n / \partial U$  and  $D = \partial D / \partial U$  near the metal-insulator transition are characterized by the exponents  $p$ ,  $q$  and  $r$  defined below.

We consider the metal-insulator phase boundary illustrated in Fig. 2. Two routes approaching the transition point at  $(\mu_c; U_c)$  indicated by the two arrows are now the subject of the present study: One is  $U \rightarrow U_c$  at  $\mu = \mu_c$  and the other is  $\mu \rightarrow \mu_c$  at  $U = U_c$ .

At  $U = U_c$ , the relation between  $n$  and  $\mu$  was already given in eq. (16), while the double occupancy as a function of  $\mu$  near  $\mu_c$  may be similarly assumed as

$$D = c \left( \frac{\mu}{\mu_c} \right)^{1-p} + D_{hf} \quad \text{for } \mu < \mu_c; \\ D_{hf} \quad \text{for } \mu > \mu_c = 0; \quad (19)$$

Here  $D_{hf}$  is the double occupancy at half filling (in the one-dimensional Hubbard model,  $D_{hf}$  is analytically cal-

culated in ref.<sup>21</sup>).

The most dominant term for the filling as a function of  $U$  near  $U_c$  is assumed in the following form:

$$n = \begin{cases} a(U_c - U)^{1-q} + 1 & \text{for } U < U_c; \\ 1 & \text{for } U > U_c; \end{cases} \quad (20)$$

At  $\mu = \mu_c$ , the double occupancy as a function of  $U$  near  $U_c$  may be assumed in the following scaling form:

$$D = \begin{cases} d(U_c - U)^{1-r} + D_{hf}(U_c) & \text{for } U < U_c; \\ D_{hf}(U) & \text{for } U > U_c; \end{cases} \quad (21)$$

In the metallic phase, the following equations are derived from eq. (19) and eq. (20), respectively:

$$\frac{\partial D}{\partial \mu} = c(1-p) \left( \frac{\mu}{\mu_c} \right)^{-p}; \quad (22)$$

$$\frac{\partial n}{\partial U} = a(1-q) (U_c - U)^{-q}; \quad (23)$$

From eq. (21) the doublon susceptibility is written as

$$D_{\frac{1}{2}} = d(1-r) (U_c - U)^{-r} \quad \text{for } U < U_c; \quad (24)$$

$$D_{\frac{1}{2}} = \frac{\partial D_{hf}(U)}{\partial U} \quad \text{for } U > U_c; \quad (25)$$

In the following, the coefficients  $a$ ,  $c$ , and  $d$ , and the critical exponents  $p$ ,  $q$  and  $r$  are derived analytically. Let us first consider eq. (19). From eq. (15), the ground-state energy is obtained by integrating over  $n$ :

$$E(\mu) = E_{hf}(\mu_c) + \frac{1}{6} \mu^3; \quad (26)$$

From this equation, the double occupancy is obtained as

$$D = \frac{\partial E}{\partial U} = D_{hf} \left( \frac{\partial}{\partial U} \right) \frac{1}{6 \mu^2} \left( \frac{\partial \mu}{\partial U} \right)^3; \quad (27)$$

Now we consider the vicinity of half filling in the metallic phase and expand  $D$  up to the first-order in terms of  $\mu$ . By substituting eq. (16) to eq. (27),  $D$  is expressed by

$$D = D_{hf} \left( \frac{\partial}{\partial U} \right)^p \frac{1}{2} \left( \frac{\mu}{\mu_c} \right)^{1-2}; \quad (28)$$

for the most dominant term. By differentiating  $D$  by  $\mu$ , we obtain

$$\frac{\partial D}{\partial \mu} = \frac{r}{2} \left( \frac{\partial}{\partial U} \right)^p \left( \frac{\mu}{\mu_c} \right)^{1-2} \quad (29)$$

for the most dominant term. Comparing eq. (29) with eq. (22), we obtain the relation between the coefficients  $c$  in eq. (19) and  $r$ :

$$c = \frac{p}{2} \left( \frac{\partial}{\partial U} \right)^p; \quad (30)$$

and the critical exponent is obtained as  $p = 1-2$ .

Second, let us consider eq. (20). Starting from eq. (16), we obtain

$$\frac{\partial n}{\partial U} = \frac{1}{2} \left( \frac{\partial}{\partial U} \right)^q \left( \frac{\mu}{\mu_c} \right)^{1-2} \\ + \frac{r}{2} \left( \frac{\mu}{\mu_c} \right)^{1-2} \left( \frac{\partial \mu}{\partial U} \right); \quad (31)$$

in the metallic side around  $(\mu_c; U_c)$ . Here, we consider the

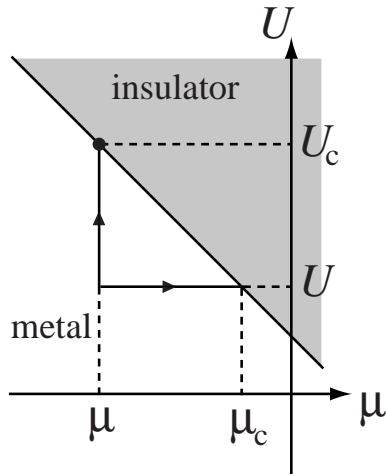


Fig. 3. Two ways of approaching the metal-insulator transition point denoted by the black circle at  $(\mu_c; U_c)$  in the  $-U$  plane: One is  $U \rightarrow U_c$  at  $\mu = \mu_c$  and the other is  $\mu \rightarrow \mu_c$  at  $U = U_c$ . These are the routes from the metallic side. The shaded area is the insulating phase and the solid line is the phase boundary.

point  $(\mu; U)$  close to the phase boundary as in Fig. 3. If we define the slope of the phase boundary near  $(\mu_c; U_c)$ , the following relation is obviously satisfied:

$$(\chi_c)_{j=U_c} = \frac{\partial}{\partial U} (U_c - U)_{j=\mu_c} : \quad (32)$$

In eq. (31), in the limit of  $\mu \rightarrow \mu_c$ , the second term is dominant and by using the relation, eq. (32), the diverging part is written as

$$\frac{\partial n}{\partial U} = \frac{\partial}{\partial U} = \frac{r}{2} \frac{\partial}{\partial U} (U_c - U)^{1/2} : \quad (33)$$

Then, the coefficient  $a$  in eq. (20) and eq. (23) is expressed by and the slope of the metal-insulator boundary:

$$a = \frac{p}{2} \frac{\partial}{\partial U} (U_c - U)^{1/2} ; \quad (34)$$

and the critical exponent is obtained as  $q = 1/2$ .

Third, let us consider eq. (21). By the derivative of both sides of eq. (28) by  $U$ , the doublon susceptibility is written as

$$\begin{aligned} \frac{\partial D}{\partial U} &= \frac{\partial D_{hf}}{\partial U} = \frac{\partial^2}{\partial U^2} \frac{p}{2} (\chi_c)^{1/2} \\ &= \frac{\partial}{\partial U} \frac{1}{2} \frac{\partial}{\partial U} (\chi_c)^{1/2} \\ &= \frac{\partial}{\partial U} \frac{1}{2} (\chi_c)^{-1/2} : \quad (35) \end{aligned}$$

Here  $(\partial^2 = \partial^2 / \partial U^2)_c$  is the curvature of the phase boundary. In the limit of  $\mu \rightarrow \mu_c$ , the most dominant term is the third term of the right-hand side of eq. (35), and by using eq. (32), we obtain

$$D = \frac{\partial D}{\partial U} = \frac{r}{2} \frac{\partial}{\partial U} (U_c - U)^{1/2} : \quad (36)$$

Then, the coefficient  $d$  in eq. (21) and eq. (24) is expressed by and the slope of the metal-insulator boundary:

$$d = \frac{p}{2} \frac{\partial}{\partial U} (U_c - U)^{3/2} ; \quad (37)$$

and the critical exponent is obtained as  $r = 1/2$ .

By eqs. (30), (34) and (37) we have derived the dominant terms of  $(\partial D = \partial)_{j=U_c}$ ,  $(\partial n = \partial U)_{j=\mu_c}$  and  $D = (\partial D = \partial U)_{j=\mu_c}$  near the Mott transition, starting from the singularity of  $\chi_c$ . Next, let us discuss the relationship between the coefficients of these terms and the slope of the metal-insulator boundary, and test Theorem 1.

### 3.2 Examination of the thermodynamic relations

From eqs. (30), (34) and (37), the following relation is derived:

$$\frac{\partial U}{\partial \chi_c} = \frac{p}{2} \frac{a}{c} = \frac{a}{d} = \frac{a}{c} : \quad (38)$$

So far, it is shown that the coefficients  $a$ ,  $c$  and  $d$  are expressed by and  $(\partial = \partial U)_c$  as in eqs. (30), (34) and (37), and the relation of eq. (38) is satisfied. To examine the thermodynamic relations of eq. (11) and eq. (12), let us focus on eq. (13): In the metallic phase,  $\partial n = \partial U$  and  $\partial D = \partial$  are continuous and hence eq. (13) holds. In the vicinity of the metal-insulator boundary,  $\partial n = \partial U$  and  $\partial D = \partial$  have the form of eq. (22) and eq. (23) and the equation holds:

$$a(U_c - U)^{1/2} = c(\chi_c - \chi)^{1/2} : \quad (39)$$

By using the relation of eq. (32), the following limit is taken in eq. (39):

$$\begin{aligned} &\lim_{U \rightarrow U_c} a(U_c - U)^{1/2} \\ &= \lim_{U \rightarrow U_c} c \frac{\partial}{\partial U} (U_c - U)^{1/2} : \quad (40) \end{aligned}$$

We see that this equation is satisfied by eq. (38). This implies that eq. (13) holds in the limit to the metal-insulator boundary from the metallic phase in the  $-U$  plane as it should be

$$\lim_{U \rightarrow U_c} a(U_c - U)^{1/2} = \lim_{\chi \rightarrow \chi_c} c(\chi_c - \chi)^{1/2} : \quad (41)$$

By using eq. (41), eq. (38) is rewritten as

$$\begin{aligned} \frac{\partial U}{\partial \chi_c} &= \frac{\lim_{\chi \rightarrow \chi_c} \frac{p}{2} (\chi_c - \chi)^{1/2}}{\lim_{U \rightarrow U_c} a(U_c - U)^{1/2}} ; \\ &= \frac{\lim_{\chi \rightarrow \chi_c} c(\chi_c - \chi)^{1/2}}{\lim_{U \rightarrow U_c} d(U_c - U)^{1/2}} : \quad (42) \end{aligned}$$

This demonstrates how the thermodynamic relations of eq. (11) and eq. (12) with a simultaneous diverging of the charge compressibility and the doublon susceptibility hold. Then, the validity of the thermodynamic relations is confirmed analytically in the case with  $\chi_c = \frac{p}{2} (\chi_c - \chi)^{1/2}$  which is known to be realized in the one- and two-dimensional Hubbard models.

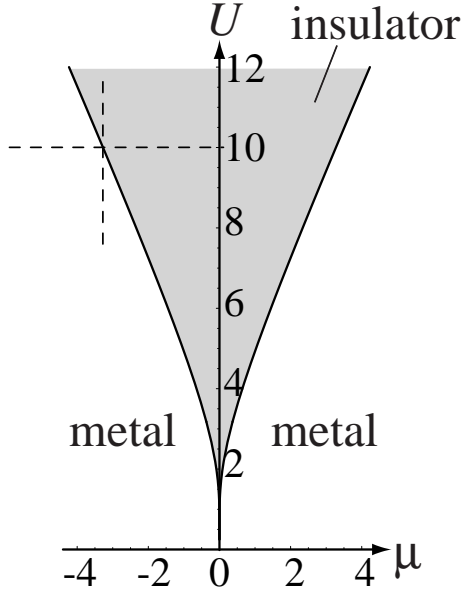


Fig. 4. Ground-state phase diagram of the one-dimensional Hubbard model for  $t = 1$ . The metal-insulator phase boundary is obtained by the Bethe-Ansatz solutions.<sup>19)</sup>

### 3.3 Bethe-Ansatz solutions in one-dimensional Hubbard model

In the one-dimensional system, the exact solutions of the Hubbard model are available by the Bethe-Ansatz equations.<sup>11,19,21)</sup> The energy and the double occupancy at zero temperature for the given filling and Coulomb interaction were calculated in ref.<sup>21)</sup> and the coefficient of the charge compressibility in eq. (15) was obtained in ref.<sup>11)</sup> The chemical potential at which the metal-insulator transition occurs for  $U$  is given by

$$\mu_c = \frac{U}{2} \frac{Z_1}{2t-1} \int_0^1 dw \frac{J_1(w)}{w(1+e^{Uw/2})}; \quad (43)$$

where upper(lower) sign denotes the electron(hole)-doped regime and  $J_1(w)$  is the first Bessel function.<sup>19)</sup> The ground-state phase diagram of the one-dimensional Hubbard model is shown in Fig. 4. By using the exact expressions of  $D$  in eqs. (2.14) and (2.15) in ref.<sup>21)</sup> and  $n$  in eqs. (6a) and (6b) in ref.<sup>11)</sup> we plot the critical behaviors of these quantities as functions of  $\mu$  and  $U$  near the Mott transition. As a typical example, we show the critical behaviors of  $n$  and  $D$  around the Mott transition point,  $(\mu_c; U_c) = (-3.277; 10.0)$  (see Fig. 4).

The chemical-potential dependence of the double occupancy for  $\mu = \mu_c$  is shown in Fig. 5. We also plot  $D = D_{hf} + \frac{p}{2} (\mu - \mu_c)^{1/2} (U_c - U)^{1/2}$  obtained from eqs. (28) and (30) by the dashed line. We see that  $\partial D / \partial \mu$  diverges at  $\mu = \mu_c$ , whose critical behavior is described by eq. (29).

The interaction dependence of the filling for  $\mu = \mu_c$  is shown in Fig. 6. We also plot  $n = 1 - \frac{p}{2} (\mu - \mu_c)^{1/2} (U_c - U)^{1/2}$  obtained from eqs. (20) and (34) by the dashed line. We see that  $\partial n / \partial U$  diverges at  $U = U_c$ , whose critical behavior is described by eq. (33).

The interaction dependence of the double occupancy

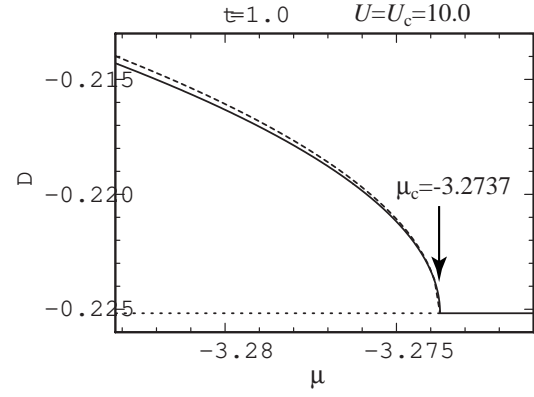


Fig. 5. Double occupancy  $D$  vs. chemical potential  $\mu$  obtained by the Bethe-Ansatz solutions of the one-dimensional Hubbard model for  $t = 1$  at  $U = U_c = 10$ . Dashed line represents  $D = D_{hf} + \frac{p}{2} (\mu - \mu_c)^{1/2} (U_c - U)^{1/2}$ .

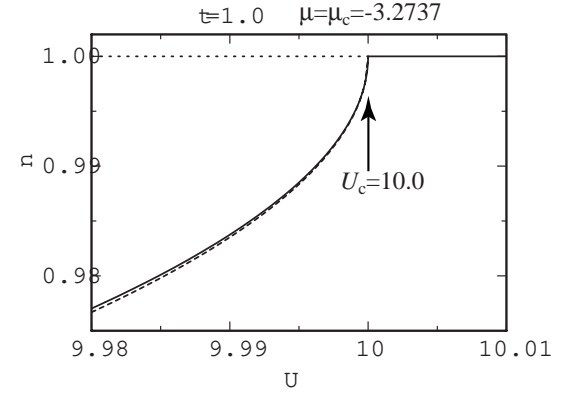


Fig. 6. Filling  $n$  vs. Coulomb interaction  $U$  obtained by the Bethe-Ansatz solutions of the one-dimensional Hubbard model for  $t = 1$  at  $\mu = \mu_c = -3.2737$ . Dashed line represents  $n = 1 - \frac{p}{2} (\mu - \mu_c)^{1/2} (U_c - U)^{1/2}$ .

for  $\mu = \mu_c$  is shown in Fig. 7. We also plot  $D = D_{hf} + \frac{p}{2} (\mu - \mu_c)^{3/2} (U_c - U)^{1/2}$  obtained from eqs. (21) and (37) by the dashed line. We see that the double occupancy diverges at  $U = U_c$  and its critical behavior is described by eq. (36).

In the one-dimensional Hubbard model, the limits of  $\mu$  in eq. (15) were shown as  $\mu \rightarrow 0$  for  $U \rightarrow 0$  and  $\mu \rightarrow 1/(2t)$  for  $U \rightarrow 1$ .<sup>11)</sup> Since  $(\mu - \mu_c) \rightarrow 0$  for  $U \rightarrow 0$  and  $(\mu - \mu_c) \rightarrow 1/2$  for  $U \rightarrow 1$ , the limits of  $a, c$  and  $d$  are as follows:  $a \rightarrow 0, c \rightarrow 0$ , and  $d \rightarrow 0$  for  $U \rightarrow 0$ , and  $a \rightarrow 1/(2t), c \rightarrow 1/(2t)$  and  $d \rightarrow 1/(2t)$  for  $U \rightarrow 1$ .

### 3.4 General expressions in d-dimensional systems with dynamical exponents $z$

We have discussed the analytic forms of  $\mu_j = \mu_c$ ,  $(\partial n / \partial U)_j = \mu_c$ ,  $(\partial D / \partial \mu)_j = \mu_c$  and  $D_j = \mu_c$ , which are realized in the one- and two-dimensional Hubbard models. Here we present the general expressions of these quantities in d-dimensional systems.

Based on the hyperscaling analysis, the critical behavior of physical quantities near the continuous filling-



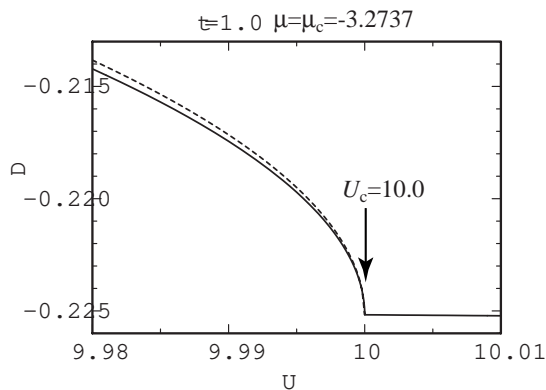


Fig. 7. Double occupancy  $D$  vs. Coulomb interaction  $U$  obtained by the Bethe-Ansatz solutions of the one-dimensional Hubbard model for  $t = 1$  at  $\mu = \mu_c = -3.2737$ . Dashed line represents  $D = D_{hf} + \frac{p}{2} \left( \frac{dU}{dc} \right)^3 (U_c - U)^{1/2}$ .

control Mott transition was predicted in ref.<sup>22)</sup> For example, the charge compressibility has the form of

$$\chi_c = \frac{r}{2} \left( \frac{dU}{dc} \right)^{(d+z)-2}; \quad (44)$$

where  $r$  is the correlation-length exponent which satisfies  $z = 1$  with  $z$  being the dynamical exponent, and  $d$  is the spatial dimension. It is known that for the usual one-dimensional Hubbard model, where  $d = 1$ , the dynamical exponent is given by  $z = 2$ , then the charge compressibility has the form of  $\chi_c \propto \left( \frac{dU}{dc} \right)^{1/2}$  as in eq. (18). For the two-dimensional system,  $d = 2$ , the dynamical exponent  $z = 4$  was identified by numerical calculations,<sup>23,24)</sup> and then the same critical behavior for  $\chi_c$  as the  $d = 1$  case appears. For the three-dimensional system, in the case of  $z = 4$ , the charge compressibility has the form of  $\chi_c \propto \left( \frac{dU}{dc} \right)^{1/4}$  by eq. (44). In the following, we show the analytic forms of the physical quantities defined by the second derivative of the Hamiltonian in general form, which are derived from eq. (44):

$$\begin{aligned} \frac{\partial n}{\partial U} = \chi_c &= \frac{r}{2} \frac{\partial}{\partial U} \left( \frac{dU}{dc} \right)^{(d+z)-1} \\ &= \frac{r}{2} \frac{\partial}{\partial U} \left( \frac{dU}{dc} \right)^{(d+z)-2} \left( \frac{dU}{dc} \right); \\ \frac{\partial D}{\partial U} &= \frac{r}{2} \frac{\partial}{\partial U} \left( \frac{dU}{dc} \right)^{(d+z)-2} \\ &= \frac{r}{2} \frac{\partial}{\partial U} \left( \frac{dU}{dc} \right)^{(d+z)-1} \left( \frac{dU}{dc} \right)^{-1} \\ &= \frac{r}{2} \frac{\partial}{\partial U} \left( \frac{dU}{dc} \right)^{(d+z)-2} \left( \frac{dU}{dc} \right)^{-1} \left( \frac{dU}{dc} \right)^2; \end{aligned}$$

The coefficients of each term are expressed by the coefficients of  $\chi_c$  and the slope of the metal-insulator boundary. The exponents are the same as that of the charge compressibility, i.e.,  $(d+z)-2$ . Note that the relation eq. (38) still holds in this case, and this implies that eq. (38) does not depend on the exponent in the divergence of the charge compressibility. This is ascribed to

the fact that thermodynamic relations of eq. (11) and eq. (12) hold in any spatial dimensions.

#### 4. Finite temperature

##### 4.1 Generalization of thermodynamic relations to finite temperature

In §3, the thermodynamic relations are examined at zero temperature. It should be noted, however, that the thermodynamic relations of eqs. (8), (11) and (13) hold even at finite temperature, if  $\langle \dots \rangle$  is taken as the thermal average:

$$\langle A \rangle = \frac{\text{tr } e^{-H/T} A}{\text{tr } e^{-H/T}}; \quad (45)$$

where  $A$  is an operator for a physical quantity and  $T$  is temperature. Hence, when temperature is fixed, in the plane of  $\langle D \rangle$  and  $U$  with the finite length of the metal-insulator boundary, eqs. (8), (11) and (13) hold.

##### 4.2 Constraints on the shape of the phase diagram for finite-temperature first-order metal-insulator transition

We also discuss the phase diagram with the temperature dependence. Starting from the expansion of the Gibbs free energy  $G(T; U)$  for electrons along the first-order metal-insulator-transition line, we obtain

$$\frac{U}{T} = \frac{S_I}{D_I} - \frac{S_M}{D_M}; \quad (46)$$

where the entropy of electrons is defined by  $S$

$(\partial G / \partial T)_U$  and  $D$  is the double occupancy in the thermal average. In experiments, when the pressure  $p$  is applied to the system, the bandwidth of the electronic system,  $U = t$  changes. Hence, in eq. (46),  $U$  corresponds to  $p$  and the double occupancy  $D$  is related to the conjugate variable, the volume  $v$ . The similarity between the metal-insulator transition and the liquid-gas transition was pointed out in ref.<sup>25)</sup>

We discuss the consequence of eq. (46). Let us consider the case that the first-order metal-insulator transition takes place in the  $U$ - $T$  phase diagram and the insulator phase has the ordering such as the magnetic one. In the metallic phase, at small but nonzero particle-hole excitations induce the entropy stemming from the finite density of states at the Fermi level, while in the insulator phase the entropy is rather small if the symmetry breaking with small degeneracy is realized while the particle-hole excitation cannot induce the entropy under the finite charge gap. Then, this yields  $S_I - S_M < 0$  and by using the fact that  $D_I - D_M < 0$ , the slope should be

$T = U > 0$  (see Fig. 8(a)). This is a reasonable result, since the metallic phase appears in the high-temperature side to govern the  $TS$  term in the free energy. This situation can be realized in the three-dimensional system, since Mermin-Wagner's theorem<sup>26)</sup> allows the magnetic ordering at finite temperature.

In the two-dimensional system, the magnetic ordering at finite temperature is suppressed by thermal fluctuation.<sup>26)</sup> In this case, the paramagnetic insulator phase can be realized for finite-temperature regime above the magnetically-ordered insulator phase at  $T = 0$ . Although

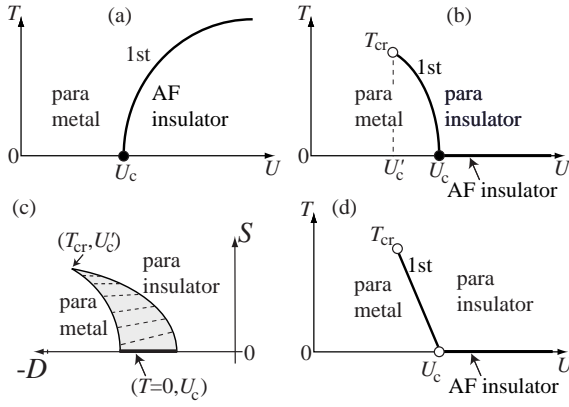


Fig. 8. Some examples of schematic phase diagrams with first-order metal-insulator transition in the plane of temperature  $T$  and Coulomb interaction  $U$ . (a): Paramagnetic metal and antiferromagnetic insulator phases in the three dimensional system. (b): Paramagnetic metal phase for  $T = 0$ , the antiferromagnetic insulator phase at  $T = 0$  and the paramagnetic insulator phase for  $T > 0$  in the two dimensional system. Open circle in (b) represents critical end point,  $T_{cr}$ , of the first-order transition line. (c): Phase diagram in the plane of double occupancy  $D$  and entropy  $S$  corresponding to (b). Gray area represents the phase-separated region between metal and insulator along the first-order-transition line in (b). Dashed line represents each set of  $(T; U)$  on the first-order-transition line in (b). (d): Schematic phase diagram for the continuous transitions both at  $T = 0$  and  $T = T_{cr}$  drawn by open circles, while the first-order transition occurs for  $0 < T < T_{cr}$ . In this case, a finite slope  $(\partial T / \partial U)_{T=0} \neq 0$  is allowed in contrast to (a) and (b) (see text).

it depends on each system how the entropy is released by the inter-site interaction in the paramagnetic-insulator phase, we refer ref.<sup>27)</sup> as an example of the appearance of the paramagnetic insulator phase at high-temperature side, i.e.,  $T = U < 0$  by  $S_M - S_I > 0$  (see Fig. 8(b)).

Let us focus on the slope of the first-order transition in the zero-temperature limit;  $(\partial T / \partial U)_{T=0}$ . When the first-order metal-insulator transition occurs at  $T = 0$ , the jump of the double occupancy appears at  $U = U_c$ , i.e.,  $D_I - D_M \neq 0$ . By the requirement of the thermodynamic third law, the entropy at  $T = 0$  should be 0 in the metal and insulator phases, and hence  $S_I = 0 = S_M$  at  $T = 0$ . Therefore, from eq. (46), the following conclusion is derived: In the phase diagram with temperature  $T$  and control parameter  $U$ , the first-order transition line should have the infinite slope in the zero-temperature limit:  $(\partial T / \partial U)_{T=0} = \infty$ . This statement is not restricted to the case of the metal-insulator transition, but can be applied to the first-order transition between any types of the phases. The schematic phase diagram in the plane of the double occupancy  $D$  and entropy  $S$  corresponding to Fig. 8(b) is illustrated in Fig. 8(c). The gray area represents the phase-separated region between the metal and the insulator along the finite-temperature first-order transition line in Fig. 8(b). The dashed line in Fig. 8(c) indicates each set of  $(T; U)$  on the finite-temperature first-order transition line in Fig. 8(b).

Here, the relationship to the known results should be mentioned. In the infinite-dimensional Hubbard model

with the fully frustrated lattice, the  $T$ - $U$  phase diagram was obtained.<sup>28,29)</sup> The first-order transition between the paramagnetic metal and the paramagnetic insulator takes place at finite temperature. One might consider that the first-order-transition line has a finite slope as  $(\partial T / \partial U)_{T=0} < \infty$  in the phase diagram, which is different from the above statement. However, at  $T = 0$  the metal-insulator transition takes place as the continuous one in that model, to which the above discussion cannot be applied. Actually, in this case, the continuous transition with  $D_I - D_M = 0$  occurs at  $T = 0$ . Then, the finite slope is possible;  $(\partial T / \partial U)_{T=0} < \infty$ . The schematic phase diagram in the  $U$ - $T$  plane for such a case is illustrated in Fig. 8(d): At  $T = 0$  and  $T = T_{cr}$ , the continuous metal-insulator transitions take place, while the first-order transition occurs for  $0 < T < T_{cr}$ .

At  $T = 0$ , possible shapes of the phase diagram with the first-order and continuous quantum phase transitions have been classified in ref.<sup>18)</sup> In the plane of the chemical potential and the Coulomb interaction  $U$ , the  $U$ -shaped phase boundary with a finite length of the first-order transition can exist, but the  $V$ -shaped phase is allowed to have the only first-order-transition point at the corner and have the continuous transitions at the edges. The  $V$ -shaped phase as an essential singular form of the Mott gap,  $\exp[-t/(U_c - U)]$  is classified into the same class as the  $V$ -shaped case.

For the  $U$ -shaped case at  $T = 0$ , a possible  $T$ - $U$ -phase diagram is illustrated in Fig. 9(a). The surface of the first-order transition is formed as drawn by the gray area in Fig. 9(a) and at the critical end curve drawn by the solid line, which describes  $T_{cr}$ , the charge compressibility diverges.<sup>30)</sup> For the  $V$ -shaped case at  $T = 0$ , the possible  $T$ - $U$ -phase diagram is illustrated in Fig. 9(b). In this case, at  $T = 0$  the first-order transition occurs at the corner of the  $V$ -shaped boundary. At finite temperatures, one possibility is that the jump of the double occupancy at  $T = 0$  disappears for infinitesimal temperature. Actually one can consider such a function for  $D(D_0; U; T)$  with  $D_0$  the chemical potential at half filling: An example is the functional form analogous to the Fermi distribution function,  $f(\epsilon; T) = 1 / [\exp(\epsilon / T) + 1]$ . At  $T = 0$  the jump of  $f(\epsilon; T)$  at  $\epsilon = 0$  appears, while at infinitesimal  $T$ , the jump disappears. This is the case illustrated in Fig. 9(b) where  $T_{cr}$  becomes zero temperature, i.e., the quantum tricritical point. In this case,  $D(D_0; U; T = 0)$  as a function of  $U$  has a jump at the bandwidth-control Mott transition point,  $U_{c0}$ , and the jump disappears at  $U_{c0}$  for  $T \neq 0$ .

The other possibility is that the jump in  $D(D_0; U; T)$  remains even for  $T \neq 0$ . In this case, the first-order-transition line, but not the surface as in Fig. 9(a), has a certain length from  $T = 0$  to  $T = T_{cr}$ . This seems to be unusual, but such a case is not ruled out by the thermodynamic argument.

## 5. Application of thermodynamic relation to general models

In x2, we have derived the thermodynamic relations for the metal-insulator transition, and in x3 we have examined that physical quantities defined by the sec-



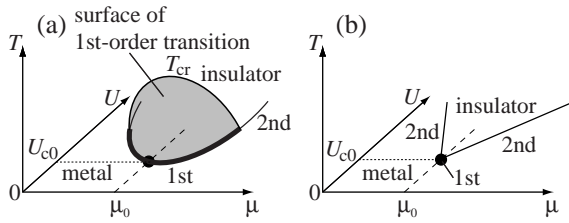


Fig. 9. Possible schematic phase diagrams in the parameter space of temperature  $T$ , chemical potential  $\mu$  and interaction  $U$  for (a)  $U$ -shaped and (b)  $V$ -shaped Mott-insulator phases at  $T = 0$ . In (a), thick (thin) line represents the first-order (continuous) transition line. Gray surface represents the surface of the first-order transition and its upper edge is the critical temperature,  $T_{cr}$ . In (a) and (b), the solid circle represents the band-width control Mott transition point at  $U_{c0}$ , and  $\mu_0$  represents the chemical potential at half filling at  $U = U_{c0}$ . The dashed line connected to  $\mu_0$  is the route of the band-width control. In (b), the first-order transition takes place only at the band-width-control Mott transition point, i.e.,  $T_{cr} = 0$ .

ond derivative of the Hamiltonian for  $\mu$  and  $U$  actually satisfy the thermodynamic relations in the cases of the one- and two-dimensional Hubbard models. However, the thermodynamic relation between the slope of the phase boundary and physical quantities defined by the first and second derivative of the Hamiltonian for the first-order and continuous transitions, respectively, can be derived in general in the other models with any types of phases in the same way as in x2.

As an example, let us consider the phase diagram whose control parameters are the on-site Coulomb interaction  $U$  and the nearest-neighbor Coulomb interaction  $V$ . The Hamiltonian is described by the extended form as

$$H_{ex} = H + V \sum_{\langle i,j \rangle} n_i n_j; \quad (47)$$

where  $\langle i,j \rangle$  denotes the nearest-neighbor sites.

At quarter filling, the existence of two phases, namely, metallic and charge-ordering phases has been reported in the one-dimensional system.<sup>31)</sup>

At the first-order transition, by expanding the ground-state energy by  $U$  and  $V$  in a similar way to the derivation of eq. (8), the slope of the phase boundary is expressed as

$$\frac{U}{V} = \frac{R_{j_1}}{D_{j_1}} \frac{R_{j_2}}{D_{j_2}}; \quad (48)$$

where

$$R = \frac{1}{N} \frac{\partial \langle H \rangle}{\partial V} = \frac{1}{N} \sum_{\langle i,j \rangle} n_i n_j; \quad (49)$$

Here, at the first-order transition, the slope of the phase boundary in the  $U$ - $V$  plane is expressed by the ratio of the jump of the nearest-neighbor correlation and the double occupancy.

At the continuous transition, the slope of the phase boundary is expressed in two ways: One is the expansion of the double occupancy and the other is the nearest-neighbor correlation. The resultant thermodynamic rela-

tions are

$$\begin{aligned} \frac{V}{U} &= \frac{D_{j_1}}{U_M} \frac{D_{j_2}}{U_I}; \\ &= \frac{R_{j_1}}{U_M} \frac{R_{j_2}}{U_I}; \end{aligned} \quad (49)$$

where the susceptibility for the nearest-neighbor correlation is defined by

$$\chi = \frac{\partial^2 \langle H \rangle}{\partial V^2}; \quad (50)$$

If  $(\partial D / \partial V)_U$  and  $(\partial R / \partial U)_V$  are continuous at  $(U; V)$ , the following relation holds, which is shown in the same way as in the derivation of eq. (13):

$$\frac{\partial D}{\partial V}_U = \frac{\partial R}{\partial U}_V; \quad (51)$$

When we add the axis of the chemical potential to the phase diagram in the plane of  $U$  and  $V$ , the thermodynamic relations in the  $-U$  plane and the  $-V$  plane can be derived as in a parallel way to x2.

Here, we show the thermodynamic relations for the first-order and continuous transitions in the extended Hubbard model as an example. It should be noted that the thermodynamic relations can also be applied to other systems in a similar way. Hence, we remark that the thermodynamic relations derived in this paper have generality. The applicability of the relations is not restricted to the specific model, but to any types of the models with the phase diagram. This is a consequence of the extensions of the Clausius-Clapeyron and Ehrenfest relations to microscopic models.

## 6. Summary

We have analytically derived several useful thermodynamic relations of the charge compressibility and the doublon susceptibility to the slope of the metal-insulator phase boundary in the plane of the chemical potential and the Coulomb interaction  $U$ . By using this relation, we have shown that the charge compressibility divergence at the metal-insulator transition causes simultaneous divergence of the doublon susceptibility when the metal-insulator transition takes place as a continuous one with a finite length and a finite and nonzero slope in the  $-U$  plane. This statement holds at any spatial dimensions and at any temperatures. The main results of the obtained relations are eqs. (11), (12) and (14).

In one- and two-dimensional Hubbard models, critical divergence of the charge compressibility at the Mott transition appears generally with the form of  $\chi_c = \frac{1}{2} (\chi_c)^{1-2}$ . Starting from this critically divergent form of  $\chi_c$ , analytical expressions of  $(\partial D / \partial V)_{U=U_c}$ ,  $(\partial n / \partial U)_{V=V_c}$  and  $D_{j_1} = \chi_c$  in the vicinity of the Mott transition are derived. All the coefficients of the most divergent terms of these quantities are expressed by the coefficient of the charge compressibility,  $\chi_c$ , and the slope of the metal-insulator boundary,  $(U = U_c)$ . All the exponents of the divergence of these quantities have the same value as the exponent of  $\chi_c$ : namely,  $1-2$ . The relations among the coefficients of  $\chi_c$  at  $U=U_c$ ,  $(\partial D / \partial V)_{U=U_c}$ ,  $(\partial n / \partial U)_{V=V_c}$  and

$\partial j = 0$  at the metal-insulator-transition point actually satisfy the thermodynamic relations derived above, i.e.,

$$\left(\frac{\partial n}{\partial U}\right)_M^2 = \left(\frac{\partial D}{\partial U}\right)_M^2 = c(D_M - D_I).$$

The above statement holds at any points of the U-shaped metal-insulator boundary and at the points of the V-shaped boundary except the corner, which is the bandwidth-control Mott transition point. At the corner of V- and -shaped phases ( $U = 0$ ) is not well defined.

By applying the above argument to the phase diagram in the parameter space of the temperature  $T$  and the interaction  $U$ , constraints on the phase boundary are classified at finite temperatures. It is shown that the infinite slope of the first-order-transition line has the infinite slope as  $(\partial T / \partial U)_{j=0} = 1$  from the requirement of the thermodynamic third law and thermodynamic relations.

These conclusions described above are not restricted only to the Hubbard model, but also can be applied to other general models. As an example, we demonstrate the derivation of the thermodynamic relations in the extended Hubbard model with the next-neighbor repulsion.

#### Acknowledgment

One of the authors (S.W.) would like to thank Prof. Minoru Takahashi, Prof. Masao Ogata and Dr. Masahiro Shiroishi for helpful suggestions about the Bethe-Ansatz solutions of the one-dimensional Hubbard model. The work is supported by Grant-in-Aid for young scientists, No. 15740203 as well as Grant-in-Aid No. 16340100 from the Ministry of Education, Culture, Sports, Science and Technology, Japan. A part of our computation has been done at the Supercomputer Center in the Institute for Solid State Physics, University of Tokyo.

1) N.F. Mott and R. Peierls: Proc. Phys. Soc. London. A 49 (1937)

72.

- 2) For review, see M. Imada, A. Fujimori and Y. Tokura: Rev. Mod. Phys. 70 (1998) 1039.
- 3) K. Kanoda: Physica C 282-287 (1997) 299.
- 4) A. Casey, H. Petel, J. Nyeki, B. P. Cowan and J. Saunders: Phys. Rev. Lett. 90 (2003) 115301, and references therein.
- 5) P. Linerette, A. Georges, D. Jerome, P. W. Zietek, P. Metcalfe and J. M. Honig: Science 302 (2003) 3.
- 6) F. Kagawa, T. Itou, K. Miyagawa and K. Kanoda: Phys. Rev. B 69 (2004) 064511 and private communication.
- 7) G. Kotliar: G. Euro. J. Phys. B :27 (1999) 11.
- 8) M. J. Rozenberg, R. Chitra and G. Kotliar: Phys. Rev. Lett. 83 (1999) 3498.
- 9) G. Kotliar, E. Lange and M. J. Rozenberg: Phys. Rev. Lett. 84 (2000) 5180.
- 10) For review, see A. Georges, G. Kotliar, W. Krauth and M. J. Rozenberg: Rev. Mod. Phys. 68 (1996) 13.
- 11) T. Ueki, N. Kawakami and A. Okiji: Phys. Lett. 135A (1989) 476.
- 12) N. Furukawa and M. Imada: J. Phys. Soc. Jpn. 61 (1992) 3331.
- 13) N. Furukawa and M. Imada: J. Phys. Soc. Jpn. 62 (1993) 2557.
- 14) T. Kashima and M. Imada: J. Phys. Soc. Jpn. 70 (2001) 3052.
- 15) H. Morita, S. Watanabe and M. Imada: J. Phys. Soc. Jpn. 71 (2001) 2109.
- 16) M. Imada and T. Kashima: J. Phys. Soc. Jpn. 69 (2000) 2723.
- 17) T. Kashima and M. Imada: J. Phys. Soc. Jpn. 70 (2001) 2287.
- 18) S. Watanabe and M. Imada: J. Phys. Soc. Jpn. 72 (2004) 1251.
- 19) L. H. Lieb and F. Y. Wu: Phys. Rev. Lett. 20 (1968) 1445.
- 20) J. E. Hirsch: Phys. Rev. B 31 (1985) 4403.
- 21) H. Shiba: Phys. Rev. B 6 (1972) 930.
- 22) M. Imada: J. Phys. Soc. Jpn. 64 (1995) 2954.
- 23) F. F. Assaad and M. Imada: J. Phys. Soc. Jpn. 65 (1996) 189.
- 24) F. F. Assaad and M. Imada: Phys. Rev. Lett. 76 (1996) 3176.
- 25) C. Castellani, C. Di Castro, D. Feinberg and J. Ranninger: Phys. Rev. Lett. 43 (1979) 1957.
- 26) N. D. Mermin and H. Wagner: Phys. Rev. Lett. 17 (1966) 1133.
- 27) S. Onoda and M. Imada: Phys. Rev. B 67 (2003) 161102.
- 28) A. Georges and W. Krauth: Phys. Rev. B 48 (1993) 7167.
- 29) M. J. Rozenberg, G. Kotliar and X. Y. Zhang: Phys. Rev. B 49 10181.
- 30) G. Kotliar, S. Murthy and M. J. Rozenberg: Phys. Rev. Lett. 82 (2002) 046401.
- 31) F. Mila and X. Zotos: Europhys. Lett. 24 (1993) 133.